LS- 157
W. Chou and J. Bridges
Jan 9, 1989
(Rev. September 4, 1990)

3-D Computer Simulations of EM Fields in the APS Vacuum Chamber — Part 1: Frequency-Domain Analysis

The vacuum chamber proposed for the storage ring of the 7-GeV Advanced Photon Source (APS) basically consists of two parts: the beam chamber and the antechamber, connected to each other by a narrow gap, as shown in Fig. 1. A sector of 1-meter-long chamber with closed end plates, to which are attached the 1-inch-diameter beampipes centered at the beam chamber, has been built for experimental purposes. The 3-D code MAFIA [1] has been used to simulate the frequency-domain behaviors of EM fields in this setup. The results are summarized in this note and are compared with that previously obtained from 2-D simulations and that from network analyzer measurements. As we will see, they are in general agreement. A parallel analysis in the time-domain is reported in a separate note. [2]

The method of our simulations can be briefly described as follows. The 1-inch-diameter beampipes are terminated by conducting walls at a length of 2 cm. The whole geometry can thus be considered as a cavity. The lowest RF modes of this geometry are computed using MAFIA. The eigenfrequencies of these modes are a direct output of the eigenvalue solver E3, whereas the type of each mode is determined by employing the postprocessor P3. The mesh sizes are chosen such that they are small enough for computations in the frequency region in which we are interested (the sampling theorem), while the total number of mesh points is still well within the range that our computer system can cope with.

Three types of boundaries have been employed in our simulations.

1. One half of the structure is used (Fig. 2). The $y = 0$ plane is a metallic boundary (conductivity $\sigma = \infty$).
2. Same as 1, but the $y = 0$ plane is a magnetic boundary (permeability $\mu = \infty$).
3. A quarter of the structure is used (Fig. 3). The $y = 0$ plane is magnetic and the $z = 0$ plane metallic.

By making use of the symmetries embedded in this geometry, not only does one save memory space, but one can also select the RF modes that are to be studied. [3] The latter will become obvious when we take a look at the attached mode tables.

The first few dozens of the lowest RF modes computed by MAFIA are listed in Tables 1, 2 and 3, corresponding to the three types of boundary conditions above. As illustrations, Figs. 4, 5 and 6 exhibit the field pattern of several modes.

With the boundary condition 1, the tangential components of the E-field near the $y = 0$ plane are zero. This implies that the major component of E is E_y and that the H-field is in the z-x plane. Therefore, the lowest modes of the vacuum chamber are of the TE_{m0p} type (in which $m, n = 0$ and p are the number of half-waves in the x, y and z direction, respectively), as shown in Table 1.

With the boundary condition 2, on the other hand, the tangential components of the H-field near the $y = 0$ plane are zero. In this case, **H** can be either in the y-z plane, which corresponds to the TE_{0np} (or higher) modes with E_x as the major E-component, or in the x-y plane, which corresponds to the TM_{m1p} (or higher) modes with E_z as the major E-component. The former (i.e., TE_{0np} modes) have lower frequencies because the dimension of the structure in the z-direction is larger than that in the x-direction. Furthermore, neither E_x nor E_z could exist in the narrow gap when frequencies are below its cutoff (about 15 GHz). Therefore, the TE_{0np} modes in the beam chamber and that in the antechamber would not be coupled at low frequencies, as shown in Table 2.

The total number of modes with the boundary condition 3 should be half of that with the boundary condition 2, due to the symmetry condition imposed on the $z = 0$ plane. When comparing Table 2 with Table 3, we see small differences in the frequencies for the same modes. This reflects the accuracy limit of the MAFIA code.

In the MAFIA output, certain missing modes are noticed and identified, e.g., TE_{012} of the beam chamber in Table 2 and TE_{0112} of the antechamber in Table 3.

For higher modes, the contamination of the fields becomes a serious problem. It is difficult to recognize the types of these modes. This is why there are some question marks in Table 2.

The 2-D code SUPERFISH was previously used to compute the TM_z and TE_z modes in the vacuum chamber when it is treated as a waveguide. [4] Some of the results are listed in Table 4. For a 1-meter-long section with closed end plates, the eigenfrequencies of RF modes, f_{mnp}, can be readily obtained from using the formula

$$f_{mnp} = [f_{mn}^2 + (pc/2L)^2]^{1/2} \tag{1}$$

in which f_{mn} are the frequencies of the waveguide modes, $L = 1\ m$ the length of the cavity, c the velocity of light, and $p = 0$ (for TM only), $1, 2, ...$ an integer. Frequencies calculated by using Eq. (1) and Table 4 are also listed in Table 1. It is seen that these results are a bit higher than that obtained directly from the 3-D simulations. This may be attributed to two causes: (a) The existence of the 2-cm-long beampipes lowers the frequencies (Slater's perturbation theorem); (b) The 3-D simulations are less accurate.

The waveguide frequencies of the TE_{01} mode of the beam chamber and the antechamber have not been calculated. Assuming the 3-D results in Table 2 are correct, one can then use Eq. (1) to compute $f(TE_{01})$, which are also included in Table 2.

Network analyzer measurements have been performed on the 1-meter-long sector of vacuum chamber. Fig. 7 shows the first few measured TE_{10p} peaks for $p = 1, 3, 5, 7, 9$ and 11. Compared with the frequencies listed in Table 1, the agreement is to one's satisfaction.

In summary, the 3-D calculations in the frequency-domain provide us with a useful list of the RF modes in the APS vacuum chamber. These results are consistent with those previously obtained from 2-D simulations as well as those from network analyzer measurements.

We have been benefited from discussions with Dr. J. Cook.

References

[1] T. Weiland, IEEE Trans. Nucl. Sci., NS-32, 2738 (1985).

[2] W. Chou, *3-D Computer Simulations of EM Fields in the APS Vacuum Chamber — Part 2: Time-Domain Analysis*, ANL Light Source Note LS- (1990).

[3] Y. Jin, *Mode Selection and Boundary Conditions Using MAFIA in Frequency-Domain*, ANL Light Source Note LS-125 (Sept. 1988).

[4] J. Cook, private communication. Also see R. L. Kustom, *Vacuum Chamber Impedance Measurements*, Proceedings of Impedance and Current Limitations Workshop, ESRF, Grenoble, France, Oct. 17-18, 1988.

Table 1. The Lowest Modes of the Vacuum Chamber with Metallic Boundary at the y=0 Plane

Mode No.	Mode Type(*)	Frequency/MHz(**)	SUPERFISH/MHz(***)
1	TE 1 0 1	359.636	362.174
2	TE 1 0 2	443.548	445.619
3	TE 1 0 3	555.921	557.603
4	TE 1 0 4	682.817	684.254
5	TE 1 0 5	817.490	818.794
6	TE 1 0 6	956.623	957.904
7	TE 2 0 1	1019.999	
8	TE 2 0 2	1052.506	
9	TE 1 0 7	1098.494	1099.853
10	TE 2 0 3	1104.574	
11	TE 2 0 4	1173.566	
12	TE 1 0 8	1242.146	1243.668
13	TE 2 0 5	1256.692	
14	TE 2 0 6	1351.332	
15	TE 1 0 9	1386.989	1388.770
16	TE 2 0 7	1455.215	
17	TE 1 0 10	1532.664	1534.793
18	TE 2 0 8	1566.478	
19	TE 1 0 11	1678.908	1681.498
20	TE 2 0 9	1683.636	
21	TE 3 0 1	1758.072	1876.021
22	TE 3 0 2	1777.132	1893.901
23	TE 3 0 3	1808.281	1923.332
24	TE 1 0 12	1816.863	1828.721
25	TE 3 0 4	1851.398	1963.794
26	TE 3 0 5	1913.751	2014.624

Notes: (*) Mode type TE mnp, in which m, n and p are the number of half-waves in the x, y and z direction, respectively.

(**) The frequencies listed in this column are calculated directly by 3-D MAFIA.

(***) The frequencies listed in this column are obtained by using the 2-D SUPERFISH results (see Table 4) and Eq. (1) (see text).

Table 2. The Lowest Modes of the Vacuum Chamber with Magnetic Boundary at the y=0 Plane

Mode No.	Mode Type(*)	Frequency/MHz(**)	FITTED/MHz(***)
1	(a) TE 0 1 1	3863.500	3863.51
2	(a) TE 0 1 2	3872.222	3872.22
3	(a) TE 0 1 3	3886.726	3886.70
4	(a) TE 0 1 4	3906.884	3906.88
5	(a) TE 0 1 5	3932.660	3932.68
6	(a) TE 0 1 6	3963.926	3963.98
7	(a) TE 0 1 7	4000.531	4000.65
8	(a) TE 0 1 8	4042.354	4042.55
9	(a) TE 0 1 9	4089.279	4089.52
10	(b) TE 0 1 1	4101.189	4101.19
11	(b) TE 0 1 2	(missed)	4109.40
12	(b) TE 0 1 3	4122.764	4123.05
13	(b) TE 0 1 4	4141.198	4142.08
	(a) TE 0 1 10		4141.39
14	(b) TE 0 1 5	4165.668	4166.41
15	(b) TE 0 1 6	4195.298	4195.97
	(a) TE 0 1 11		4197.97
16	(b) TE 0 1 7	4247.644	4230.63
	(a) TE 0 1 12		4259.08
17	(b) TE 0 1 8	4267.948	4270.28
18	(b) TE 0 1 9	4313.211	4314.77
19	(b) TE 0 1 10	4335.413	4363.96
	(a) TE 0 1 13		4324.52
20	(b) TE 0 1 10(?)	4364.271	4363.96
	(a) TE 0 1 14		4394.10
21	(b) TE 0 1 11	4426.653	4417.69
	(a) TE ?		
22	(b) TE 0 1 12	4479.475	4475.80
	(b) TM 1 1 1 (?)		4478.78

Notes: (*) Mode type TE mnp, in which m, n and p are the number of half-waves in the x, y and z direction, respectively.

(**) The frequencies listed in this column are calculated directly by 3-D MAFIA.

(***) The frequencies listed in this column (except the last one) are obtained by assuming the following waveguide frequencies and using Eq. (1) (see text).

f(TE01) of the beam chamber: 4098.45 MHz.
f(TE01) of the antechamber: 3860.6 MHz.

(a) The mode is confined to the antechamber.

(b) The mode is confined to the beam chamber.

When both (a) and (b) appear following the same mode number, it means that there are two different modes in the beam chamber and the antechamber, respectively, which have almost the same frequency but are not coupled.

Table 3. The Lowest Modes of the Half-Length Vacuum Chamber with Magnetic boundary at the y=0 Plane and Metallic Boundary at the z=0 Plane

Mode No.	Mode Type(*)	Frequency/MHz(**)
1	(a) TE 0 1 2	3885.101
2	(a) TE 0 1 4	3919.639
3	(a) TE 0 1 6	3976.495
4	(a) TE 0 1 8	4054.668
5	(b) TE 0 1 2	4110.493
6	(b) TE 0 1 4	4142.887
7	(a) TE 0 1 10	4152.869
8	(b) TE 0 1 6	4196.297
9	(b) TE 0 1 8	4269.681
10	(b) TE 0 1 10	4362.483
11	(a) TE 0 1 12	(missed)
12	(a) TE 0 1 14	4403.322

Notes: (*) Mode type TE mnp, in which m, n and p are the number of half-waves in the x, y and z direction, respectively.
(**) The frequncies listed in this column are calculated directly by 3-D MAFIA.
(a) The mode is confined to the antechamber.
(b) The mode is confined to the beam chamber.

Table 4. Waveguide modes from SUPERFISH(+)

	Mode Type(*)	Frequency/MHz
Vacuum chamber		
	TE 1 0	329.698
	TE 2 0	(N/A)
	TE 3 0	1870.023
	TE 4 0	2255.089
	TE 5 0	2653.074
Beam chamber		
	TM 1 1	4476.278
	TM 2 1	6086.078

Notes: (+) The calculations are done by J. Cook.
(*) Mode type TE mn, in which m and n are the number of half-waves in the x and y direction, respectively.

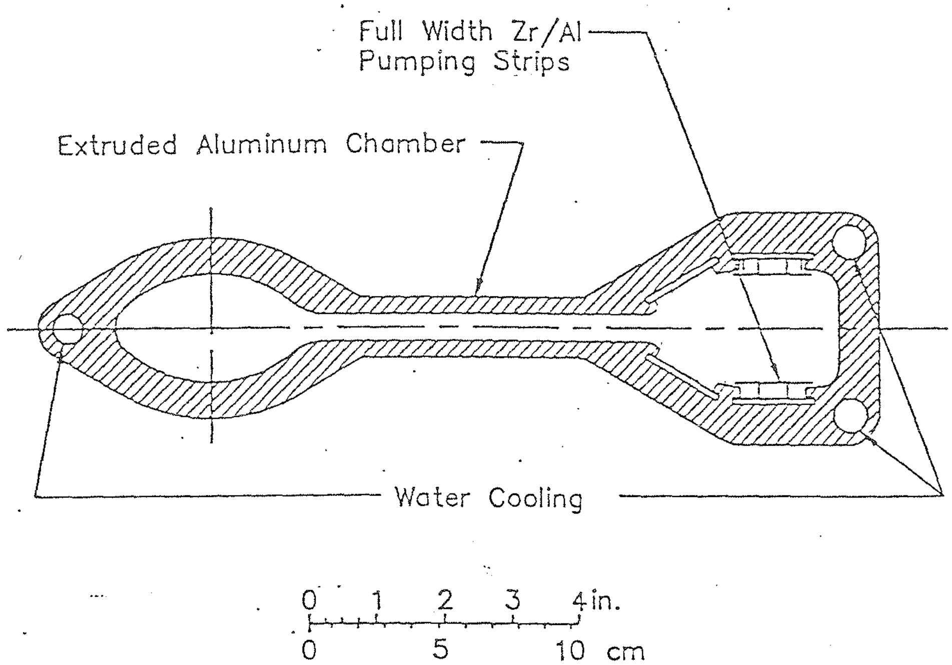

Fig. 1. The cross-section of the APS Vacuum chamber.

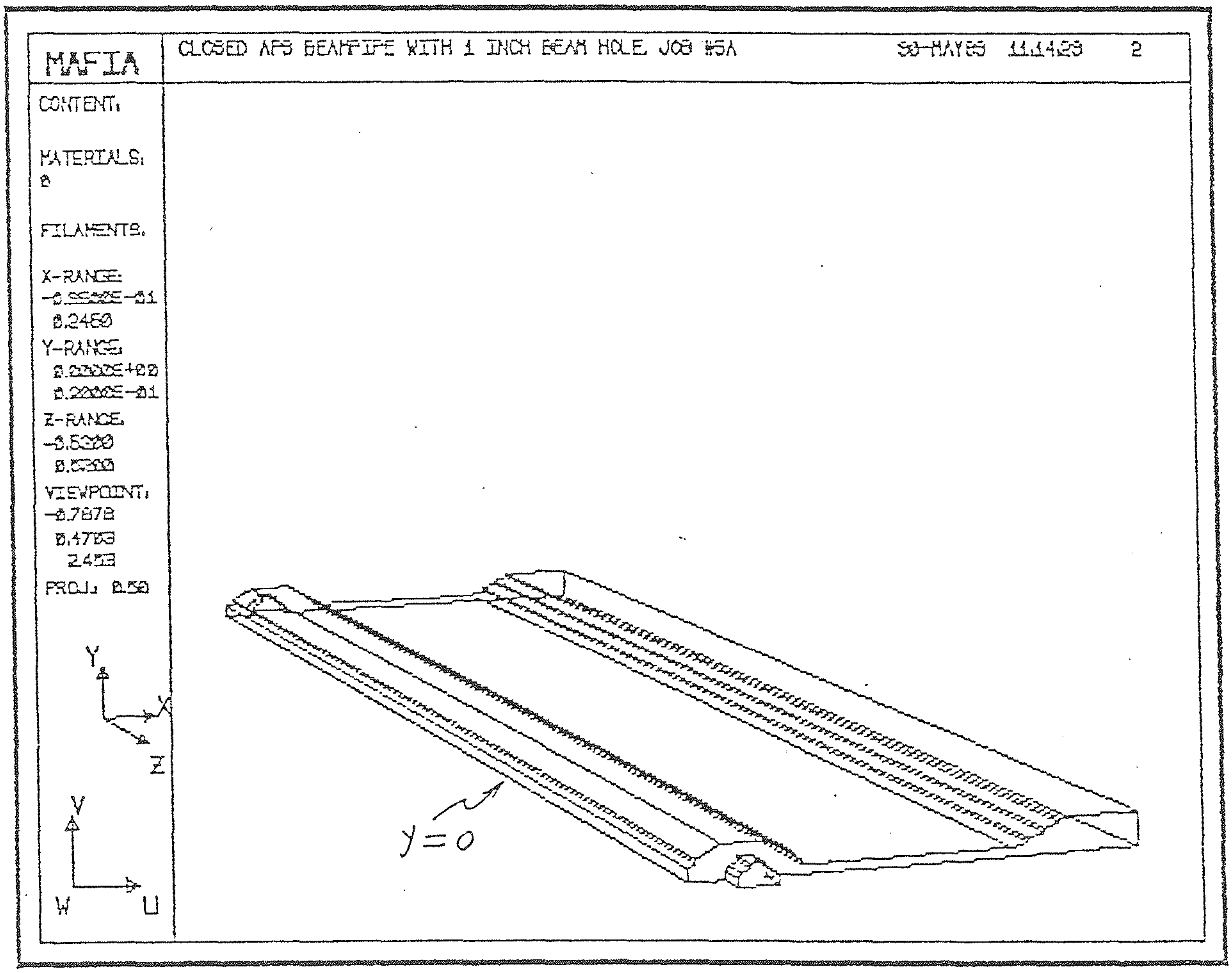

Fig. 2. One half of the vacuum chamber that is used in the simulations. The $y = 0$ plane is either a metallic ($\sigma = \infty$) or a magnetic ($\mu = \infty$) boundary.

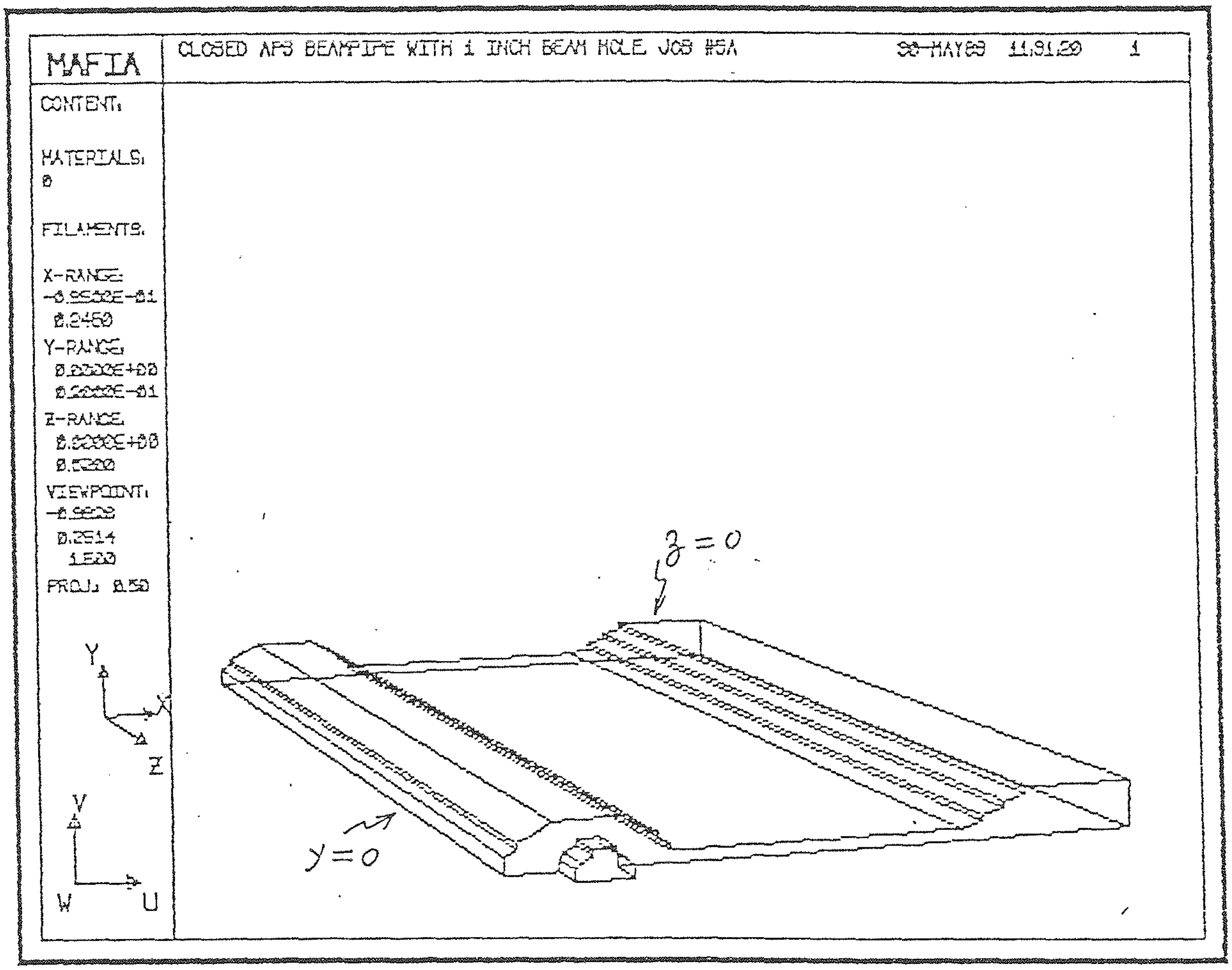

Fig. 3. One quarter of the vacuum chamber that is used in the simulations. The $y = 0$ plane is magnetic ($\mu = \infty$) and the $z = 0$ plane is metallic ($\sigma = \infty$).

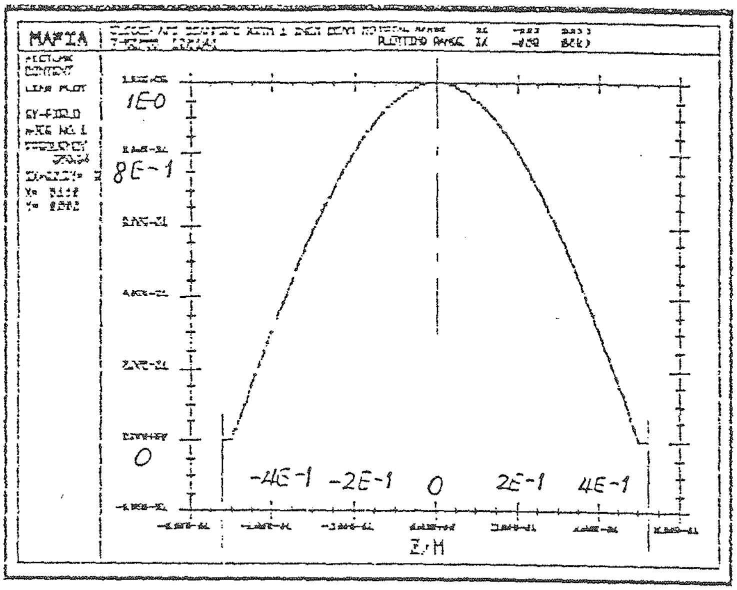

Ey along z-axis

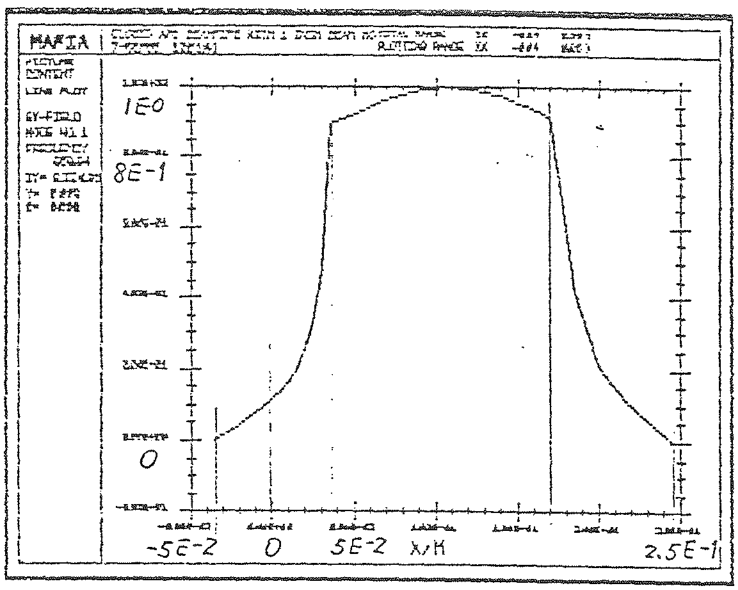

Ey along x-axis

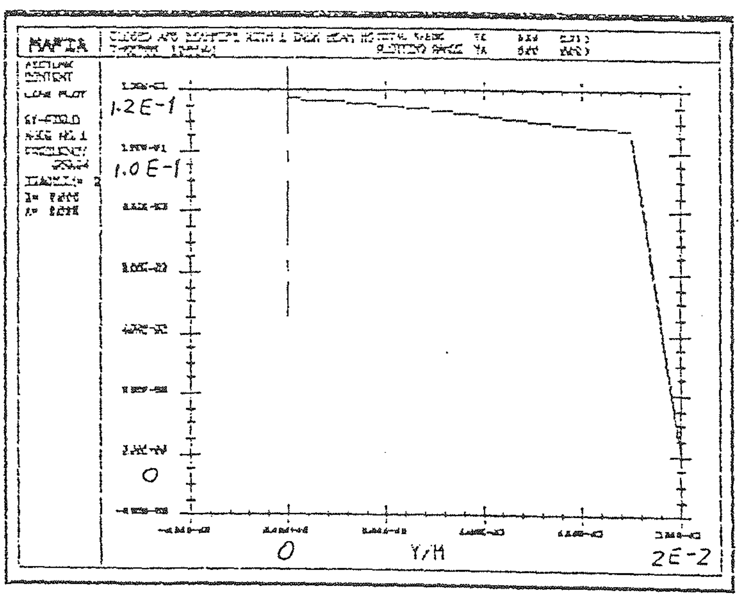

Ey along y-axis

Fig. 4. The TE_{101} mode of the 1-meter-long sector of vacuum chamber computed by MAFIA.

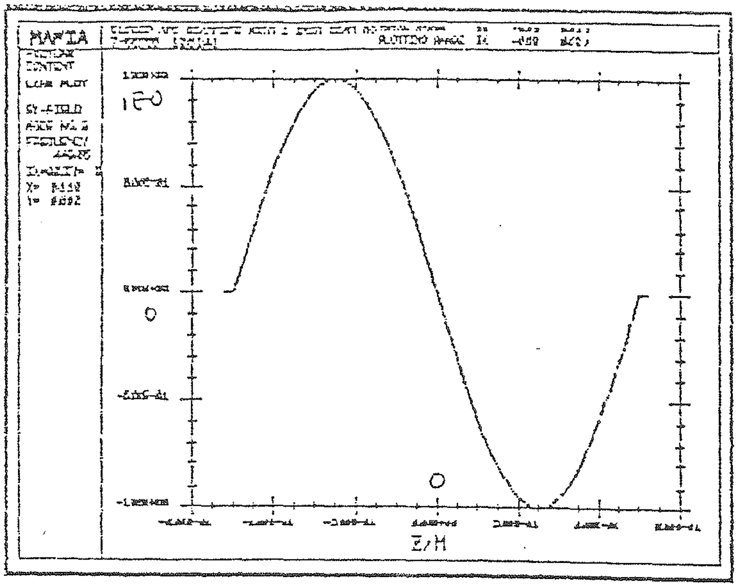

E_y along z-axis

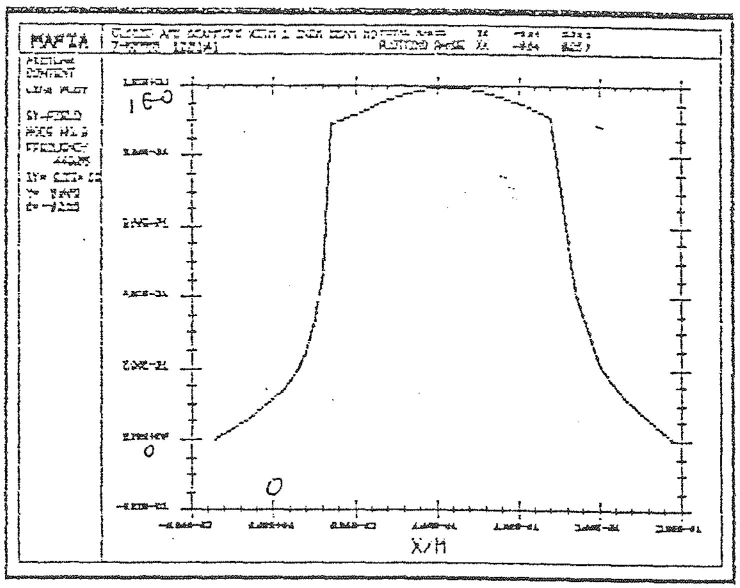

E_y along x-axis

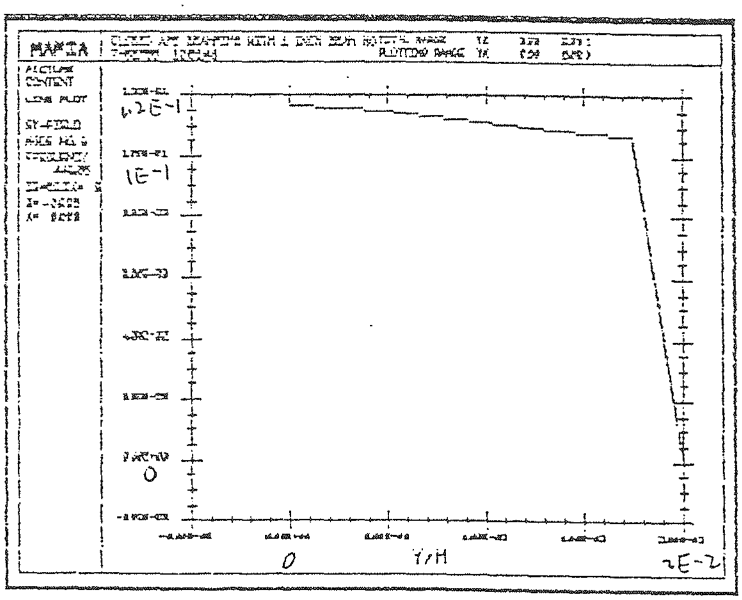

E_y along y-axis

Fig. 5. The TE_{102} mode of the 1-meter-long sector of vacuum chamber computed by MAFIA.

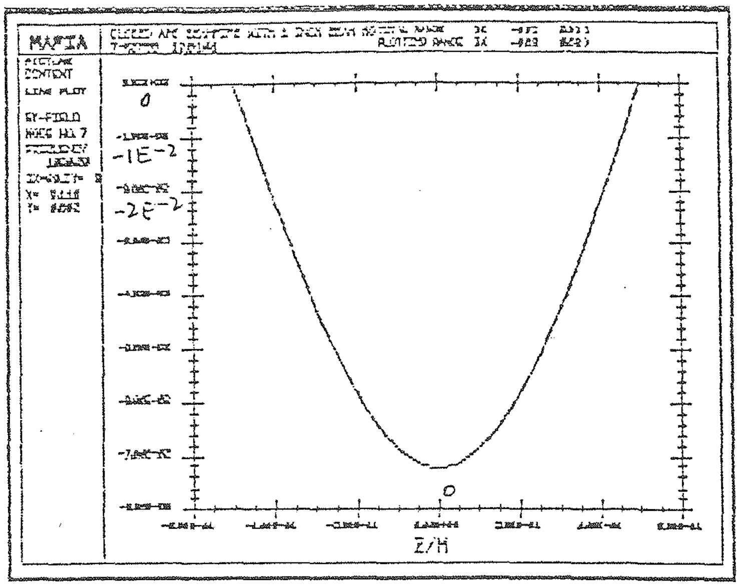

Ey along z-axis

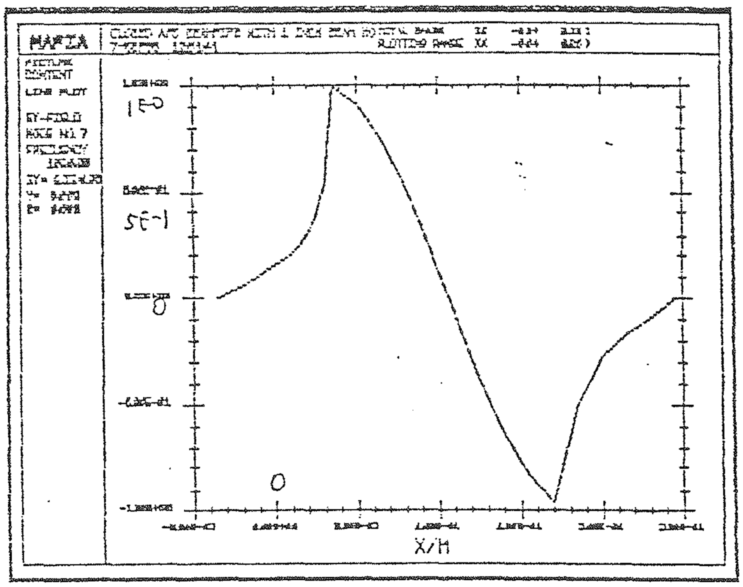

Ey along x-axis

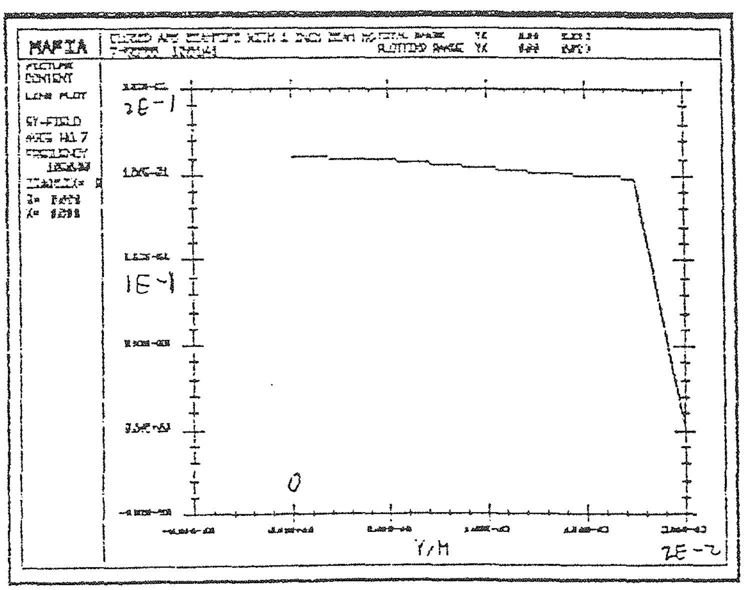

Ey along y-axis

Fig. 6. The TE_{201} mode of the 1-meter-long sector of vacuum chamber computed by MAFIA.

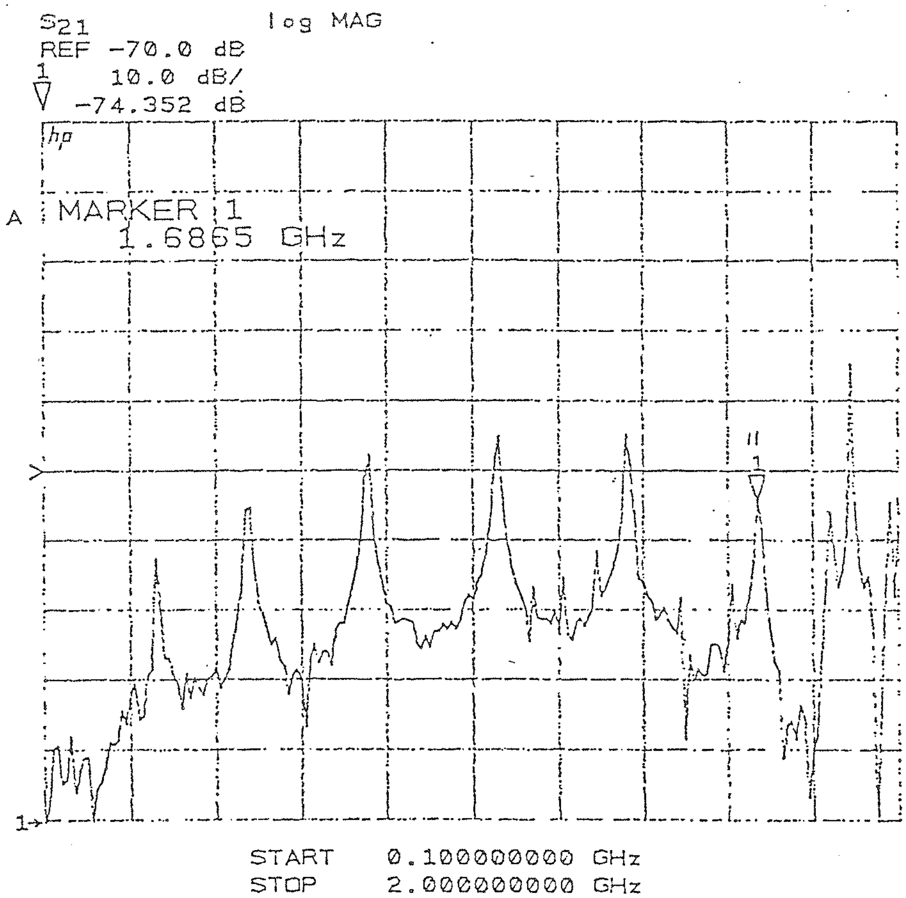

Fig. 7. The TE_{10p} ($p = 1, 3, 5, 7, 9, 11$) peaks of the 1-meter-long sector of vacuum chamber measured by a network analyzer. The marked peak is that for $p = 11$. Its measured value (1686.5 MHz) is in agreement with the calculated one listed in Table 1 (1678.9 MHz).